Tunghai Science Vol. 14: 01-18

June, 2012



# 2D HetCOR NMR Spectrum and Structure of benzyl N-ferrocenyl carbamate $CpFe(\eta^5\text{-}C_5H_4NHCOOCH_2C_6H_5)$

Yu-Pin Wang*, Jia-Chwen Wu, Hsiu-Yao Cheng, Tso-Shen Lin,

## Abstract

Ferrocenoyl azide **4** underwent Curtius rearrangement in the presence of benzyl alcohol to form a urethane derivative, benzyl N-ferrocenylcarbamate **5**. The structure of **5** has been determined by X-ray diffraction studies: space group, $P2_1/c$; monoclinic; a = 13.400(3), b = 9.811(3), c = 11.436(3) Å, β = 94.79(2); Z = 4. The exocyclic nitrogen is bent away from the iron atom with an angle θ of -2.37°. The chemical shifts of C(2,5) and C(3,4) on the Cp ring were assigned using two-dimensional HetCOR NMR spectroscopy. The electron density distribution in the cyclopentadienyl ring of the Cp(Fe) was discussed on the basis of $^{13}C$ NMR data and compared with calculations using the density functional B3LYP exchange-correlation method.

**Keywords:** Iron, Ferrocene, Carbamate, HetCOR NMR, B3LYP

# 1 Introduction

In the last few years, a steadily increasing number of systems with exciting new biological activities have been prepared by the conjugation of organometallic compounds to bio(macro)molecules [1,2]. The potential applications of these systems, including use as antitumor agents [3], antibacterial agents [4], and radiopharmaceuticals [5], have prompted us to study compound benzyl N-ferrocenylcarbamate **5**. The preparation and NMR data of **5** have been previously reported [6], however its $^{13}C$ NMR data has not been examined thoroughly. Herein, we report the 2D NMR spectra and the crystal structure of **5**. Based on the 2D HetCOR correlation spectrum, unequivocal assignments for the C(2,5) and C(3,4) of the cyclopentadienyl ring (Cp(Fe)) of **5** were made.

# 2 Results and discussion

By reacting with phosphorus pentachloride, ferrocenoic acid, **2** was transformed into CpFe($\eta^5$-$C_5H_4COCl$) **3** [7]. Without further purification, **3** reacted readily with sodium azide in acetone to afford ferrocenoyl azide **4.** Azide **4** underwent Curtius rearrangement in the presence of benzyl alcohol to form a urethane derivative, benzyl N-ferrocenylcarbamate **5,** in a yield of 48% yield.

$$\text{CpFe}(\eta^5\text{-C}_5\text{H}_4\text{-COOH})\ \mathbf{2} \xrightarrow[\text{C}_6\text{H}_6]{\text{PCl}_5} \text{CpFe}(\eta^5\text{-C}_5\text{H}_4\text{-COCl})\ \mathbf{3} \xrightarrow[\text{CH}_3\text{COCH}_3]{\text{NaN}_3} \mathbf{4}$$

$$\text{CpFe}(\eta^5\text{-C}_5\text{H}_4\text{-CON}_3)\ \mathbf{4} \xrightarrow[\text{heat}]{\text{C}_6\text{H}_5\text{CH}_2\text{OH}} \text{CpFe}(\eta^5\text{-C}_5\text{H}_4\text{-NHCOOCH}_2\text{C}_6\text{H}_5)\ \mathbf{5}$$

The $^{1}$H NMR spectrum of **5** (Table 1) exhibited a singlet cyclopentadienyl resonance at δ 4.17 corresponding to the protons of the unsubstituted Cp ring ($Cp^{2}$(Fe)). A 1H singlet at δ 5.88 owing to –NH proton and a 2H singlet at δ 5.16 owing to methylene protons were observed. The assignments for H(2–5) of the monosubstituted Cp ring ($Cp^{1}$(Fe)) were difficult to make. Based on the spectrum of the corresponding 2-deuterio compound, a pair of triplets at δ 4.03 and 4.53 were assigned to the protons H(3,4) and H(2,5) of $Cp^{1}$(Fe) [8].

From Fig. 1, it is worth to note that the broadness of downfield triplet further supports the above assignments. The observed diastereotopism of the H(2,5) and H(3,4) pairs of the Cp(Fe) ring could originate from hindered rotation about the exocyclic C(1)–N(1) bond. It reveals that there is a, to some extent, contribution of canonical form **5***i* to **5**.

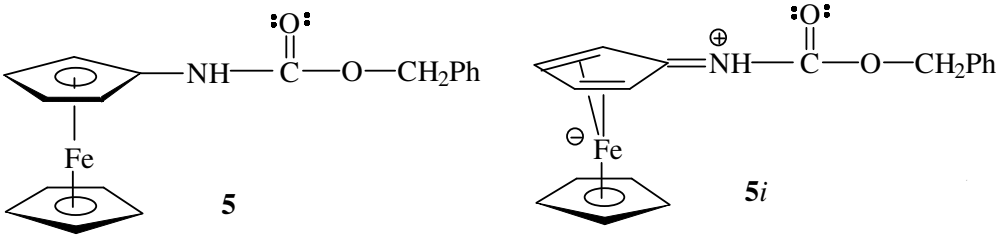


The broader triplet has been assigned to the H(2,5) protons also on the basis of the fact that the protons located nearest to the diastereotopic center (N) would be expected to show a greater diastereotopic effect, whereas a proton located at either the 3- or 4-position would show little or no diastereotopic effect.

The assignments of $^{13}$C NMR spectra for **5** were based on standard $^{13}$C NMR [9], 2D HetCOR, and DEPT correlation techniques. They were also compared with other ferrocene derivatives (Table 2) [10]. Two relatively less intense signals were observed at δ 96.21and 136.23, corresponding to the C(1) of $Cp^{1}$(Fe) and ipso carbon of phenyl ring, respectively. The methylene carbon resonates at δ 67.00. Chemical shifts at δ128.21, 128.31, and 128.61 were assigned to *m*-, *p*-, and *o*- carbon, respectively, of phenyl ring. The line assignments for the C(2–5) of Cp(Fe) were more difficult to

make. Based on the 2D HetCOR results (Fig. 1), in which the magnetic fields of $^{1}H$ and $^{13}C$ NMR spectra increase toward the right and upper side, respectively, the upfield chemical shifts of C(2,5) correlate with the downfield chemical shifts of H(2,5) (δ 4.53) and the downfield chemical shifts of C(3,4) correlate with the upfield chemical shifts of H(3,4) (δ 4.03). Accordingly, chemical shifts at δ 60.92 and 64.66 were assigned to C(2,5) and C(3,4), respectively, of $Cp^{1}$(Fe).

These assignments reveal that positions 2 and 5 on the substituted Cp ring in ferrocene are more sensitive to electron-donating substituents, as previously found for aminoferrocene (Table 2) [10].

The molecular structure of **5** is shown in Fig. 2. Selected bond distances and angles are given in Table 3. The atomic coordinates of the atoms are listed in Table 4. For the purpose of comparison, the selected structural data of **6** [11], **7** [12], and **8** (Fig. 3) [13] are also listed in Table 5.

The bond length of C(Cp)(C1)–carbamate nitrogen(N1)(1.419(17) Å) is short. Simple $C(sp^3)$–$N(sp^3)$ single-bond distances are expected to be 1.47Å [14]. Allowing for the greater s character (and therefore shorter bond length) of the $sp^2$ hybrid on Cp compared to the $sp^3$ hybrid of the methyl group by about 0.04 Å [14], we would expect the C(Cp)–$N(sp^3)$ single bond distance to be 1.43 Å. Thus, the shorter (Δ = 0.011 Å) than expected distance demonstrates that there is resonance between the carbamate nitrogen and the Cp ring.

From Table 5, two interesting features are revealed: the length of Fe--exocyclic atom in **5** is 3.154 Å (Fe--N(1)), considerably longer than 3.057Å (Fe--C) in **8,** and **8** bears a large value of positive θ (5.09°), whereas **5** bears a large value of negative θ (-2.37°). The ability of the exocyclic double bond to donate electron density to the iron atom, reestablishing the favored 18-electron count, leads to the exocyclic carbon bending towards the iron atom with an angle θ of 5.09° in the case of **8**. The θ angle is defined

as the angle between the exocyclic bond ((C(11)–C)) in **8** and (C(1)–N(1)) in **5**) and the corresponding Cp ring with a positive angle toward metal and a negative angle away from the metal.

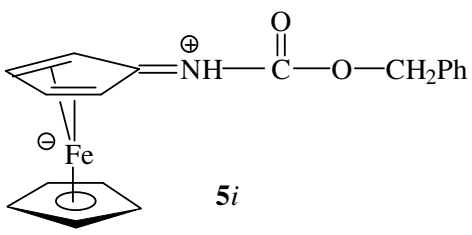


**5***i*

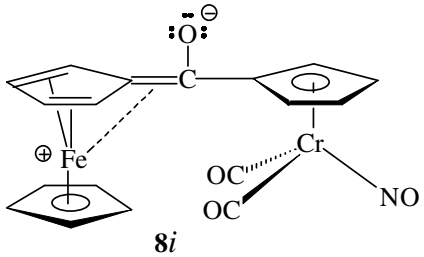


**8***i*

On the contrary, in the case of **5**, a compound with an electron-donating substituent, the exocyclic nitrogen turned away from the iron atom to minimize the repulsion between the electron rich iron and the exocyclic double bond. This leads to Fe--N distance longer than expected and a large value of negative θ.

After obtaining the X-ray structure of **5**, the charges of C(2,5) and C(3,4) for complex **5** (-0.31455 and -0.30917 for C(2,5); -0.27675 and -0.26768 for C(3,4)) were determined by ab-initio calculations using the 6-311G(d) basis set. These values correlated well with the unequivocal assignments of the $^{13}C$ chemical shifts for **5** (Table 2).

## 3 Experimental

All the syntheses were carried out under nitrogen by the use of Schlenk techniques. Traces of oxygen in the nitrogen were removed with BASF catalyst and deoxygenated nitrogen was dried over molecular sieves (3 Å) and $P_2O_5$. Hexane, pentane, benzene, and dichloromethane were dried over calcium hydride and freshly distilled under nitrogen. Diethyl ether was dried over sodium and redistilled under nitrogen from sodium-benzophenone ketyl. All the other solvents were used as commercially obtained. Column chromatography was carried out under nitrogen with Merck

Kiesel-gel 60. The silica gel was heated with a heat gun during mixing in a rotary evaporator attached to a vacuum pump for 1 h to remove water and oxygen. The silica gel was then stored under nitrogen until use. $^{1}$H- , $^{13}$C-NMR, and 2D $^{1}$H{$^{13}$C} HetCOR (HETeronuclear COrrelation) experiments were acquired on a Varian Unity-300 spectrometer. Chemical shifts were referenced to tetramethylsilane. IR spectra were recorded a Perkin-Elmer Fourier transform IR 1725X spectrophotomer. Microanalyses were carried out by the Microanalytic Laboratory of the National Chung Hsing University.

### *3.1 Preparation of benzyl-N-ferrocenyl carbamate* **5**

Phosphorus pentachloride (0.93g, 4.47 mmol) was added in two portions to a stirred solution of ferrocenoic acid **2** (0.93 g, 4.05 mmol) in 50 ml of dry benzene. The solution was stirred for 2 h at room temperature, followed by filtration through celite under nitrogen. The filtrate was concentrated under vacuum at 50°C to remove benzene and phosphorus oxychloride. Chloroformylferrocene was obtained as a brown residue. The residue was dissolved in 15 ml of acetone and treated all at once with sodium azide (0.4 g, 6.15 mmol). After stirring for 1h at room temperature, 25 ml of deoxygenated ice-water was poured into the reaction mixture, and the stirring was continued for another 15 min. The reaction mixture was then extracted with three 25 ml portions of ether. The extracts were combined and dried with anhydrous magnesium sulphate. The solution was filtered and concentrated to give azidocarbonylferrocene. Ten milliliter of benzyl alcohol was added and the solution slowly heated to 200°C. The unreacted benzyl alcohol was then evaporated under vacuum. The brownish oily residue was extracted twice with 50 ml of diethyl ether and petroleum ether. The upper organic layer was dried with anhydrous magnesium sulphate. The solution was filtered and concentrated to a yellow solid. Two grams of

silica gel were added to the solution and the solvent was removed under vacuum. The residue was added to a dry-packed column (2 cm x 10 cm) of silica gel. Elution of the column with hexane: benzene (1:3) gave a band which upon removal of the solvent under vacuum gave benzyl N-ferrocenyl carbamate **5** (0.65 g (48%)) as a red brown solid. An analytical sample, m.p. 112°C, was obtained by recrystallization using the solvent expansion method from hexane: methylene chloride (5:2) at 0°C.

Proton NMR ($CDCl_3$): $\delta$ (relative intensity, multiplicity, assignment): 4.03 (2H, t, ($Cp^1$(Fe), H(3,4)); 4.53 (2H, t, ($Cp^1$(Fe), H(2,5)); 4.17 (5H, s, $Cp^2$(Fe)); 5.16 (2H, s, -$CH_2$); 5.88 (1H, s, –NH–); 7.35 (1H, t, *p*-Ph); 7.38(2H, t, *m*-Ph); 7.39 (2H, d, *o*-Ph). Carbon–13 NMR ($CDCl_3$): δ(assignment): 60.92 ($Cp^1$(Fe), C(2,5)); 64.66 (Cp(Fe), C(3,4)); 67.00 (–$CH_2$–); 96.21 (Cp(Fe), C(1)); 128.21 (Ph, C(3,5)); 128.31 (Ph, C(4)); 128.61 (Ph, C(2,6)); 136.23 (Ph, C(1)); 153.70 (–C(O)–).

### *3.2. X-ray Diffraction analysis of 5*

The intensity data were collected on a Siemens R3m/V diffractomer with a graphite monochromator (Mo-$K_\alpha$ radiation). θ -2θ scan data were collected at room temperature (23$^o$C). The data were corrected for absorption, Lorentz and polarization effects. The absorption correction was according to the empirical psi rotation. The details of crystal data and intensity collection were summarized in Table 6.

The structures were solved by direct methods and were refined by full matrix least squares refinement based on F values. All of the non-hydrogen atoms were refined with anisotropic thermal parameters. All of the hydrogen atoms were positioned at calculated coordinate with a fixed isotropic thermal parameter (U = U(attached atom) + 0.01 Å$^2$). Atomic scattering factors and corrections for anomalous dispersion were from *International Tables for X-ray Crystallography* [15]. All calculations were performed on a PC computer using Shelex software package [16].

### *3.3 Computational Method*

Calculations based on DFT were carried out using the B3LYP hybrid method involving the three-parameter Becke exchange functional [17] and a Lee-Yang-Parr correlation functional [18]. All calculations were performed using the Gaussian 09 program [19]. The geometry for **5** was taken from the crystallographic data. The atomic charges have been analyzed using the Mulliken population analysis.

## Acknowledgements

The authors are grateful to the National Science Council of Taiwan for kindly support of this research program and the computational resources provided by the National Center for High-Performance Computing.

## References

[1] K. Splith, I. Neundorf, W. Hu, H.W. P. N'Dongo, V. Vasylyeva, K. Merz, U. Schatzschneider, Dalton Trans. 39 (2010) 2536–2545.

[2] N. Metzler-Nolte, Chimia 61 (2007) 736–741.

[3] M.A. Neukamm, A. Pinto, N. Metzler-Nolte, Chem. Commun. (2008) 232–234.

[4]J.T. Chantson, M.V.V. Falzacappa, S.Crovella, ChemMedChem 1 (2006) 1268–1274.

[5] A.F. Armstrong, N. Oakley, S. Parker, P.W. Causey, J. Lemon, A. Capretta, C. Zimmerman, J. Joyal, F. Appoh, J. Zubieta, J.W. Babich, G. Singh, J.F. Valliant, Chem. Commun. (2008) 5532–5534.

[6] A. Bertogg, F. Camponovo, A. Togni, Eur. J. Inorg. Chem. (2005) 347–356

[7] F. Rebiere, O. Samuel, H.B. Kagan, Tetrahedron Lett. 31 (1990) 3121–3124.

[8] E.W. Slocum.C.R. Ernst, Adv. Organomet. Chem. 10 (1972) 79–114.

[9] J.B. Stotter, Carbon-13-NMR Spectroscopy, Academic Press, New York, 1972, pp. 197–207.

[10] M.H. Chisholm, S. Godleshi, Prog. Inorg. Chem. (1976) 299–436.

[11] C.L. Perrine, M. Zeller, J. Woolcock, A.D. Hunter, J. Chem. Crystallogr. 35 (2005) 717–721.

[12] K. Sato, M. Katada, H. Sano, M. Konno, Bull. Chem. Soc. Jpn. 57 (1984) 2361–2365.

[13] Y.-P. Wang, J.-M. Hwu, S.-L. Wang, J. Organomet. Chem. 371 (1989) 71–79.

[14] J. March, Advanced Organic Chemistry: Reactions, Mechanisms, and Sturcture, John Wiley & Sons Inc. New York, 2007.

[15] International Tables for X-ray Crystallography, Kynoch, Birmingham, UK, Vol. IV, 1974.

[16] E.J. Gabe, Y. LePage, J.-P. Charland, F., L. Lee, P.S. White, J. Appl. Crystallogr., 22 (1989) 384–387.

[17] A.D. Becke, Density-functional thermochemistry. III. The role of exact exchange, J. Chem. Phys. 98 (1993) 5648–5653.

[18] C. Lee, W. Yang, R.G. Parr, Development of the Colle-Salvetti correlation-energy formula into a functional of the electron density, Phys. Rev. B 37 (1988) 78–789.

[19] M.J Frisch, G.W. Trucks, H.B. Schlegel, G.E. Scuseria, M.A. Robb, J.R. Cheeseman, G. Scalmani, V. Barone, B. Mennucci, G.A. Petersson, H. Nakatsuji, M. Caricato, X. Li, H.P. Hratchian, A.F. Izmaylov, J. Bloino, G. Zheng, J.L. Sonnenberg, M. Hada, M. Ehara, K. Toyota, R. Fukuda, J. Hasegawa, M. Ishida, T. Nakajima, Y. Honda, O. Kitao, H. Nakai, T. Vreven, Jr.J.A. Montgomery, J.E. Peralta, F. Ogliaro, M. Bearpark, J.J. Heyd, E. Brothers, K.N. Kudin, V.N. Staroverov, R. Kobayashi, J. Normand, K. Raghavachari, A. Rendell, J.C. Burant, S.S. Iyengar, J. Tomasi, M. Cossi, N. Rega, J.M. Millam, M. Klene, J.E. Knox, J.B. Cross, V. Bakken, C. Adamo, J. Jaramillo, R. Gomperts, R.E. Stratmann, O. Yazyev, A.J. Austin, R. Cammi, C. Pomelli, J.W. Ochterski, R.L. Martin, K. Morokuma, V.G. Zakrzewski, G.A. Voth, P. Salvador, J.J. Dannenberg, S. Dapprich, A.D. Daniels, O. Farkas, J.B. Foresman, J.V. Ortiz, J. Cioslowski, D.J. Fox, *Gaussian 09*, *Revision A.02*; Gaussian, Inc., Wallingford CT, 2009.

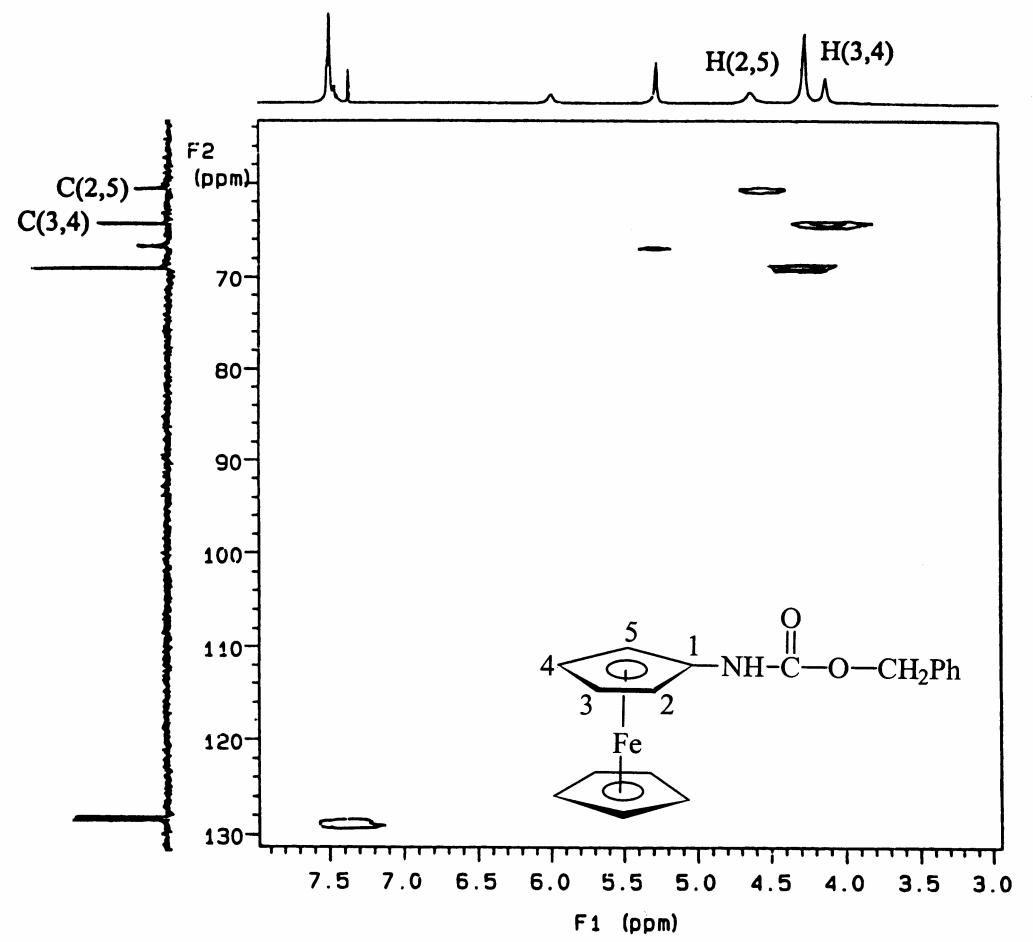


**Fig. 1.** Two-dimensional $^{1}H$-$^{13}C$ HetCOR NMR spectrum of **5** in $CDCl_3$.

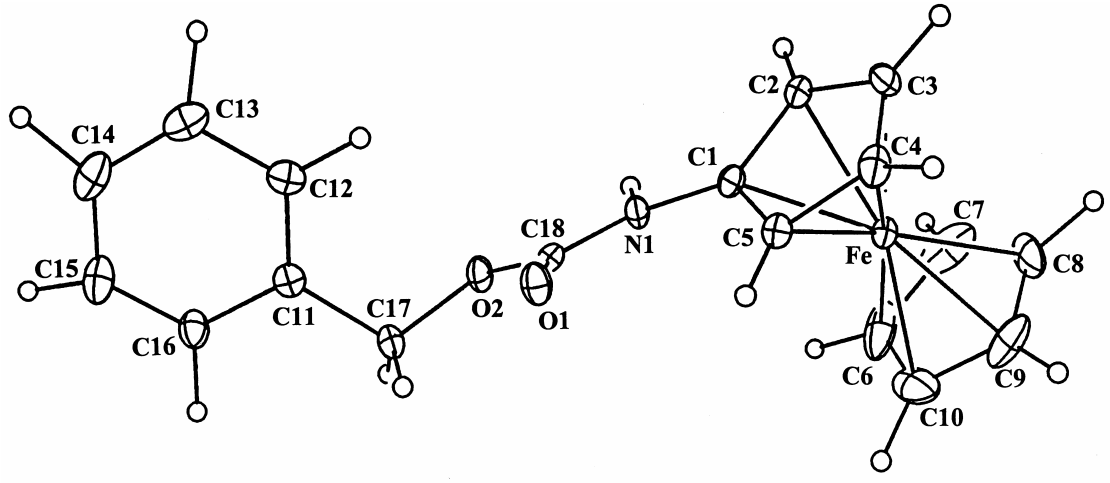


**Fig. 2.** Molecular configuration of **5**

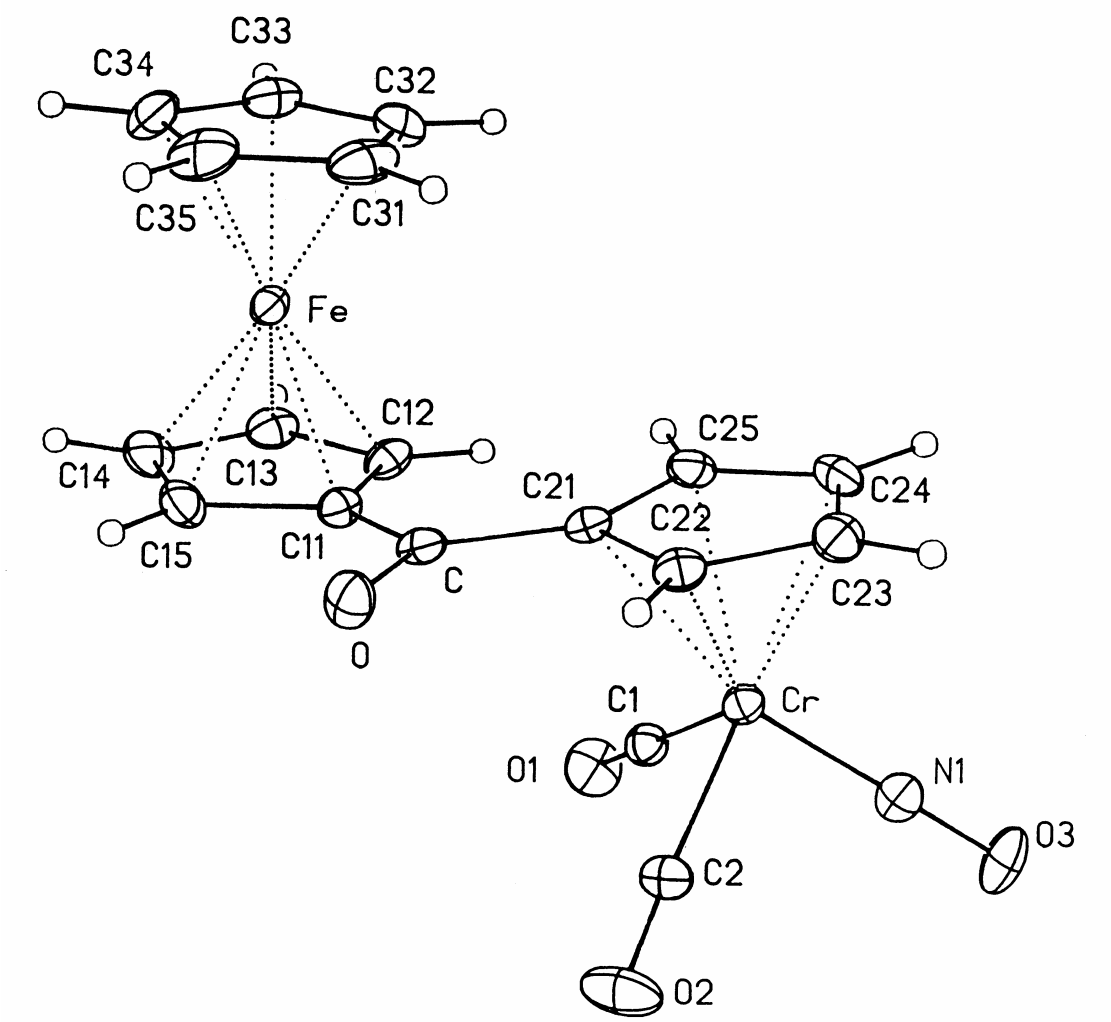


**Fig. 3.** Molecular configuration of **8**.

**Table 1**
$^{1}$H NMR data and $\Delta^{a}$

| Compound | $Cp^{1}$(Fe) δ (ppm) | | | $Cp^{2}$(Fe) | Others |
|---|---|---|---|---|---|
| | H(2,5) | H(3,4) | $\Delta^{a}$ (ppm) | | |
| FeH | 4.04 (H(1–5)) | | 0 | 4.04 | |
| $CpFe(C_5H_4\text{-}NHCOOCH_2C_6H_5)$ **5** | **4.53** | 4.03 | 0.50 | 4.17 | 5.16 ($-CH_2-$), 5.88 (–NH–), 7.35 (*p*-, Ph), 7.38 (*m*-, Ph), 7.39 (*o*-, Ph). |
| $CpFe(C_5H_4\text{-}NH_2)$ **6** | **3.99** | 3.84 | 0.15 | 4.10 | |

[a] $\Delta = \delta[H(2,5)]-\delta[H(3,4)]$
( +: H(2.5)downfield, H(3,4) upfield; – : H(2,5) upfield, H(3,4) downfield). The lower-field chemical shift of each pair is underlined.

**Table 2**
$^{13}$C{1H} NMR data and $\Delta^{a}$

| Compound | $Cp^{1}$(Fe) δ (ppm) | | | | $Cp^{2}$(Fe) | -C(O)- | Others |
|---|---|---|---|---|---|---|---|
| | C(1) | C(2,5) | C(3,4) | $\Delta^{a}$ (ppm) | | | |
| FeH | 67.90(C(1–5)) | | | | | | |
| $CpFe(C_5H_4\text{-}NHCOOCH_2C_6H_5)$ **5** | 96.21 | 60.92 | **64.66** | –3.74 | 69.42 | 153.70 | 67.00($-OCH_2-$), 128.21(*m*-, Ph), 128.31 (*p*-, Ph), 128.61 (*o*-, Ph), 136.23 (*ipso*, Ph). |
| $CpFe(C_5H_4\text{-}NH_2)$ **6** | 104.40 | 59.00 | **63.20** | –4.20 | 68.70 | | |

[a] $\Delta = \delta[C(2,5)]-\delta[C(3,4)]$
( +: C(2.5)downfield, C(3,4) upfield; – : C(2,5) upfield, C(3,4) downfield). The lower-field chemical shift of each pair is underlined.

**Table 3**
Selected bond length (Å) and selected bond angles ($^{o}$) for **5**

| | | | |
|---|---|---|---|
| Fe–C(1) | 2.065(5) | N(1)–C(1)–C(2) | 124.3(5) |
| Fe–C(2) | 2.043(5) | N(1)–C(1)–C(5) | 127.1(5) |
| Fe–C(3) | 2.030(5) | C(1)–N(1)–C(18) | 122.8(4) |
| Fe–C(4) | 2.029(6) | N(1)–C(18)–O(1) | 127.5(5) |
| Fe–C(5) | 2.042(5) | N(1)–C(18)–O(2) | 108.8(4) |
| C(1)–C(2) | 1.424(7) | O(1)–C(18)–O(2) | 123.8(5) |
| C(1)–C(5) | 1.411(7) | C(17)–O(2)–C(18) | 116.7(4) |
| C(1)–N(1) | 1.419(6) | C(11)–C(17)–O(2) | 112.4(4) |
| C(2)–C(3) | 1.409(8) | C(17)–C(11)–C(12) | 123.5(5) |
| C(3)–C(4) | 1.419(9) | C(17)–C(11)–C(16) | 117.6(4) |
| C(4)–C(5) | 1.423(8) | | |
| C(6)–C(7) | 1.412(15) | | |
| C(6)–C(10) | 1.348(17) | | |
| C(7)–C(8) | 1.392(12) | | |
| C(8)–C(9) | 1.379(12) | | |
| C(9)–C(10) | 1.354(13) | | |
| C(11)–C(12) | 1.384(7) | | |
| C(11)–C(16) | 1.400(7) | | |
| C(11)–C(17) | 1.508(7) | | |
| C(12)–C(13) | 1.406(9) | | |
| C(13)–C(14) | 1.397(10) | | |
| C(14)–C(15) | 1.385(10) | | |
| C(15)–C(16) | 1.374(8) | | |
| C(17)–O(2) | 1.447(6) | | |
| C(18)–O(1) | 1.217(7) | | |
| C(18)–O(2) | 1.357(6) | | |
| C(18)–N(1) | 1.348(7) | | |
| Fe..$Cp^{1}$(cen.) | 1.648 | | |
| Fe..$Cp^{2}$(cen.) | 1.652 | | |

| Dihedral angles between planes | |
|---|---|
| $Cp^{1}$(Fe) and carbonyl plane (N1, C18, O1, O2) | 29.38 |
| Phenyl and carbonyl plane (N1, C18,, O1, O2) | 78.47 |
| $Cp^{1}$(Fe) and phenyl | 76.22 |

**Table 4.**

Atomic coordinates ( x $10^4$) and equivalent isotropic displacement parameters ($Å^2$x $10^3$) for **5**. U(eq) is defined as one third of the trace of the orthogonalized $U^{ij}$ tensor.

| | x | y | z | U(eq) |
|---|---|---|---|---|
| Fe | 7493(1) | 1497(1) | 5802(1) | 32(1) |
| O1 | 4652(3) | 2785(4) | 7422(3) | 44(1) |
| O2 | 4545(3) | 822(3) | 8457(3) | 40(1) |
| N1 | 5508(3) | 840(4) | 6992(3) | 33(1) |
| C1 | 5982(3) | 1352(5) | 6018(4) | 32(2) |
| C2 | 6243(4) | 542(6) | 5056(5) | 41(2) |
| C3 | 6652(4) | 1415(7) | 4243(4) | 45(2) |
| C4 | 6660(4) | 2758(6) | 4705(5) | 45(2) |
| C5 | 6258(4) | 2715(5) | 5818(4) | 34(2) |
| C6 | 8299(5) | 731(13) | 7227(8) | 90(4) |
| C7 | 8565(6) | 85(7) | 6195(10) | 88(4) |
| C8 | 8943(5) | 1114(10) | 5519(6) | 71(3) |
| C9 | 8877(5) | 2342(8) | 6093(9) | 76(3) |
| C10 | 8494(6) | 2072(12) | 7127(8) | 90(4) |
| C11 | 2911(4) | 1401(5) | 9149(4) | 35(2) |
| C12 | 2403(4) | 1257(6) | 8052(5) | 49(2) |
| C13 | 1352(5) | 1177(6) | 7935(6) | 58(2) |
| C14 | 821(4) | 1264(7) | 8932(7) | 64(3) |
| C15 | 1332(4) | 1416(7) | 10029(6) | 62(2) |
| C16 | 2359(4) | 1480(6) | 10134(4) | 45(2) |
| C17 | 4034(4) | 1530(6) | 9344(4) | 42(2) |
| C18 | 4886(3) | 1599(6) | 7593(4) | 34(2) |

**Table 5**
Selected structural data of **5-8**

| Compound | | Bond length (Å) | | $\theta_M$(°)[a] | M--A[b](exocyclic) | | | | | |
|---|---|---|---|---|---|---|---|---|---|---|
| | | Fe-C(ring) | C(Cp(Fe))–A[b](exocyclic) | | | Cp | | | | |
| | | | | | | C1–C2 | C2–C3 | C3–C4 | C4–C5 | C1–C5 |
| **5** | CpFe($C_5H_4$-NHCOOCH$_2$$C_6H_5$) | 2.042(5) | 1.419(17) (C1–N1) | –2.37 | 3.154 | 1.424(7) | 1.409(8) | 1.419(9) | 1.423(8) | 1.411(7) |
| **6** | CpFe($C_5H_4$-$NH_2$) | 2.046(2) | 1.406(3) (C1–N1) | –5.51 | 3.219 | 1.422(3) | 1.428(3) | 1.418(4) | 1.427(3) | 1.420(3) |
| **7** | CpFe($C_5H_4$-$COCH_3$) | 2.038(5) | 1.493(5) (C11–C) | 2.16 | 3.116 | 1.436(6) | 1.410(6) | 1.407(7) | 1.418(6) | 1.431(6) |
| | | | | | | C11–C12 | C12–C13 | C13–C14 | C14–C15 | C11–C15 |
| **8** | CpFe($C_5H_4COC_5H_4$)Cr(CO)$_2$(NO) | 2.039(5) | 1.470(5) (C11–C) | 5.09 | 3.057 | 1.432(6) | 1.414(6) | 1.405(8) | 1.407(7) | 1.433(6) |

[a] $\theta_M$(°): the θ angle is defined as the angle between the exocyclic C-C(or N) bond and the corresponding Cp ring with a positive angle toward metal and a negative angle away from the metal.
[b] A: atom C or N.

**Table 6**
Selected crystal data and structure refinement for **5**

| | |
|---|---|
| Identification code | 920065 |
| Empirical formula | $C_{18}H_{17}FeNO_2$ |
| Color; Habit | Yellow; Lamellar |
| Formula weight | 335.2 |
| Temperature | 296 K |
| Crystal system | Monoclinic |
| Space group | $P2_1/c$ |
| Unit cell dimensions | a = 13.400(3) |
| | b = 9.811(3) Å β= 94.79(2)°. |
| | c = 11.436(3). |
| Volume | 1498.3(7) $Å^3$ |
| Z | 4 |
| Density (calculated) | 1.486Mg/$m^3$ |
| Absorption coefficient | 1.010 $mm^{-1}$ |
| F(000) | 696 |
| Crystal size | 0.44 x 0.24 x 0.06 $mm^3$ |
| Theta range for data collection | 1.25 to 25.00°. |
| Index ranges | -15<=h<=15, 0<=k<=11, 0<=l<=13 |
| Reflections collected | 2977 (1753 >= 3.0 $\sigma$ (I)) |
| Independent reflections | 2652 (1612 >= 3.0 $\sigma$ (I)) |
| No. Reflns. For Indexing | 14 (9.04° <= 2 $\theta$ <= 24.67°) |
| Diffractometer used | Siemens R3m/V |
| Radiation | MoK $\alpha$ ( $\lambda$ = 0.71073 $Å^3$ ) |
| Scan Type | $\theta$ /2 $\theta$ |
| Scan Speed | Variable; 2.44 to 14.65° /min. in $\omega$ |
| Scan Range ( $\omega$ ) | 1.00° plus K $\alpha$ -separation |
| Background Measurement | Stationary crystal and stationary |
| | Counter at beginning and end of |
| | scan, each for 25.0% of total scan time |
| Standard Reflections | 3 measured every 50 reflections |
| Hydrogen Atoms | Located on difference map |
| Weithting Scheme | w -1 = $\sigma^2$(F) + .0002$F^2$ |
| Number of Parameters refined | 199 |
| Largest and Mean $\Delta / \sigma$ | 0.001, 0.000 |
| Data-to-Parameter Ratio | 8.1:1 |
| Max. and min. transmission | 0.9877 and 0.7679 |
| Goodness-of-fit | 1.56 |
| Final R indices (obs. Data)] | R = 0.0443, Rw = 0.0428 |
| Largest diff. peak and hole | 0.28 and -0.34 e.$Å^{-3}$ |

# 化合物 CpFe($\eta^5$-$C_5H_4NHCOOCH_2C_6H_5$)二維異核 NMR 光譜及結構分析

王玉蘋*, 吳家淳, 鄭秀瑤, 林哲生

## 摘　要

化合物 Fc($CON_3$)(**4**)溶解在 $C_6H_5CH_2OH$, 之後經 Curtius 重排反應得化合物 $FcNHCOOCH_2C_6H_5$ (**5**). **5** 的結構已由 X-ray 繞射法解析出。晶體參數如下: Space group, $P2_1/c$; monoclinic; a = 13.400(3), b = 9.811(3), c = 11.436(3) Å, β = 94.79(2); Z = 4. 此環上氧醯胺基的氮的位向與 Fe 原子相反, 其 θ 角爲 –2.37°. 經由二維異核相對應 NMR 光譜儀, 化合物 $FcNHCOOCH_2C_6H_5$ **5** 的 $^{13}C$ 化學位移得以確認。文中以 B3LYP exchange-correlation 的理論計算法得出的電子密度分佈情形, 其結果呼應由 C13 NMR 化學位移所得之 Cp(Fe)的電子密度分佈狀況。

**關鍵字:** 鐵, 弗洛笙, 卡氧醯胺基, HetCOR NMR, B3LYP